BRIEF ORIGINAL COMMUNICATION

The infection fatality risk of pandemic influenza A(H1N1) in Hong Kong in 2009

Jessica Y. Wong[1], Peng Wu[1], Hiroshi Nishiura[1,2], Edward Goldstein[3], Eric H. Y. Lau[1], Lin Yang[1], SK Chuang[4], Thomas Tsang[4], J. S. Malik Peiris[1,5], Joseph T. Wu*[1], Benjamin J. Cowling*[1]

*Joint senior authors

Affiliations:

1. School of Public Health, Li Ka Shing Faculty of Medicine, The University of Hong Kong, Hong Kong Special Administrative Region, China.
2. Precursory Research for Embryonic Science and Technology, Japan Science and Technology Agency, Saitama, Japan.
3. Center for Communicable Disease Dynamics, Department of Epidemiology, Harvard School of Public Health, Boston, MA.
4. Centre for Health Protection, Department of Health, Government of the Hong Kong Special Administrative Region, Hong Kong Special Administrative Region, China.
5. Centre for Influenza Research, Li Ka Shing Faculty of Medicine, The University of Hong Kong, Hong Kong Special Administrative Region, China.

Corresponding author:

Dr Benjamin J Cowling, School of Public Health, Li Ka Shing Faculty of Medicine, The University of Hong Kong, 21 Sassoon Road, Pokfulam, Hong Kong.

Tel: +852 3906 2011; Fax: +852 3520 1945; email: bcowling@hku.hk

Word count (abstract): 189

Word count (main text): 2,002

Running head: Infection fatality risk of 2009-H1N1

Abbreviations:

pH1N1 = 2009 pandemic influenza A(H1N1)

CFR = case fatality risk

IFR = infection fatality risk

IFRc = infection fatality risk based on deaths of confirmed cases

IFRe = infection fatality risk based on excess influenza-associated deaths

CI = confidence interval

ILI = influenza-like illness

LAB = laboratory

GP = general practitioners

FUNDING

This project was supported by the Harvard Center for Communicable Disease Dynamics from the National Institute of General Medical Sciences (grant no. U54 GM088558), and the Area of Excellence Scheme of the Hong Kong University Grants Committee (grant no. AoE/M-12/06). HN received funding support from JST PRESTO program. The funding bodies had no role in study design, data collection and analysis, preparation of the manuscript, or the decision to publish.

CONFLICTS OF INTEREST

JSMP receives research funding from Crucell MV. JTW is an associate editor of AJE. BJC has received research funding from MedImmune Inc., and consults for Crucell MV. The authors report no other potential conflicts of interest.

ACKNOWLEDGMENTS

We thank Mr. Horace Choi, Ms. Vicky Fang, Dr. Andrew Ho, Ms. Kathy Leung and Dr. Irene Wong for technical support. We thank Dr. Dennis Ip and Dr. Heath Kelly for helpful discussions.

ABSTRACT

One measure of the severity of a pandemic influenza at an individual level is the risk of death among people infected by the new virus. However, there are complications in estimating both the numerator and denominator. Regarding the numerator, statistical estimates of the excess deaths associated with influenza virus infections tend to exceed the number of deaths associated with laboratory-confirmed infection. Regarding the denominator, few infections are laboratory-confirmed, while differences in case definitions and approaches to case ascertainment can lead to wide variation in case fatality risk estimates. Serologic surveillance can be used to estimate the cumulative incidence of infection as a denominator which is more comparable across studies. We estimated that the first wave of 2009-H1N1 was associated with approximately 232 (95% confidence interval: 136-328) excess deaths in all ages in Hong Kong, mainly in the elderly. The point estimates of the risk of death on a per-infection basis increased substantially with age, from below 1 per 100,000 infections in children to 1,099 per 100,000 infections in those 60-69y of age. Substantial variation in the age-specific infection fatality risk complicates comparison of the severity of different influenza strains.

Key words:

Human influenza, death, severity.

INTRODUCTION

The severity profile of a pandemic influenza virus, in combination with its transmissibility, determines the impact it will have in a population (1). One commonly reported measure of severity at the individual level is the risk of death among people infected by the virus, and this conditional measure is referred to as the case fatality risk (CFR), or sometimes the case fatality rate or ratio. There are well-known complications in quantifying both the numerator and the denominator of the CFR (2). Regarding the numerator, deaths of individuals with confirmed infection would under-ascertain all deaths associated with infection (3-6). Instead of directly counting 'confirmed' deaths, it is also possible to statistically estimate excess deaths (5-9). Regarding the denominator, most influenza infections are mild, laboratory testing has limited capacity, is expensive and often unnecessary for clinical management, and therefore few infections would be laboratory-confirmed (10, 11).

It is feasible to estimate the incidence rates of infections in a population if relevant surveillance data are available (12, 13), and the estimated cumulative incidence of infection may provide more unbiased denominators of CFR that addresses the unobservability of infection and minimizes ascertainment bias. In the present study, we propose such a severity measure referred to as the infection fatality risk (IFR), and define it as the number of influenza-associated deaths divided by the number of infections in a population or subgroup. The IFR is expected to permit comparisons (e.g. across age- and risk-groups), and we investigate the IFR where the numerator is based on deaths among individuals

with confirmed infection (abbreviated IFRc) as well as with the numerator based on statistical estimates of excess deaths (abbreviated IFRe). IFRc involves ascertainment and underreporting biases, while IFRe assumes full description of observed data by statistical modeling.

The first objective of our study was to estimate the number of excess deaths associated with the first wave of 2009 pandemic influenza A(H1N1) (hereafter denoted pH1N1) in Hong Kong. The second objective was to estimate the age-specific severity profiles of IFRc and IFRe, and to investigate the differences between them.

METHODS

Sources of Data

Age-specific all-cause deaths and the corresponding annual mid-year populations from 2001 through 2009 were obtained from the Hong Kong Government Census and Statistics Department (14, 15). Age-specific hospitalizations and deaths associated with laboratory-confirmed pH1N1 infection from 1 May 2009 through 31 December 2009 were provided by the Hong Kong Hospital Authority. Surveillance data on influenza-like illness from around 50 sentinel general practitioners were available as the weekly proportion of outpatients reporting a fever >37.8°C plus a cough or sore throat (denoted 'ILI data' hereafter), along with local laboratory data on the weekly proportion of specimens from sentinel outpatient clinics and local hospitals that tested positive for influenza (denoted 'LAB data' hereafter) (16). Surveillance

data stratified by age were not available. Data on temperature and humidity were obtained from the Hong Kong Observatory (17). Age-specific estimates of the cumulative incidence of pH1N1 infection in the first wave were estimated in separate serologic surveillance studies (18, 19), and used as the denominators for estimation of IFRc and IFRe.

Statistical Analysis

We assume that all excess deaths are truly associated with pH1N1. To address the uncertainty, four statistical models were used to estimate the excess deaths, namely time series regression, linear regression, and Poisson regression with log links and identity links. In each approach we compared excess death estimates based on four different proxy measures of local influenza activity including: (1) weekly incidence rates of pH1N1 infection, (2) weekly ILI data, (3) weekly LAB data, and (4) the product of weekly ILI and LAB data. Incidence rates of pH1N1 infection were estimated by deconvoluting the time series of hospitalizations associated with pH1N1 allowing for the delay from infection to hospitalization and scaling to serial cross-sectional serologic data (Web Appendix) (18).

We applied each regression model to the time series of weekly all-cause mortality rates from 2001 through 2009, excluding February-September 2003 which was affected by the Severe Acute Respiratory Syndrome epidemic. The data were stratified into 8 age groups: 0-4 years, 5-14y, 15-29y, 30-39y, 40-49y, 50-59y, 60-69y and ≥70y. In each regression model we included one of the measures of influenza activity as a covariate, lagged by 1 week to allow for a

delay between infection and death, and also adjusted for covariates including seasonal influenza activity, respiratory syncytial virus activity, mean temperature and absolute humidity (Web Appendix). Trigonometric components were included to allow for cyclic annual seasonality. The influenza-associated excess mortality rates were calculated by subtracting the predicted mortality rate estimated from each fitted regression model setting influenza activity as zero from the predicted mortality rate from the same model based on the observed weekly influenza activity. Further details of the statistical methods are described in the Web Appendix. All analyses were conducted in R version 2.13.1 (20).

RESULTS

The first wave of pH1N1 in Hong Kong began in the summer and peaked in September 2009 before activity declined to low levels (Figure 1). Local all-cause mortality rates generally increased in the winter, and there was no obvious increase in all-cause deaths during the peak of the pandemic (Web Appendix). Because the patterns of age-specific pH1N1 incidence rates were similar in each age group (Figure 1), we directly standardized these age-specific pH1N1 incidence rates using the Hong Kong population. The resulting age-standardized incidence rates were then used as a single proxy measure of influenza activity.

We compared the correlation between the ILI data, the LAB data, and the product of ILI and LAB data versus age-standardized incidence rates (Figure 2). ILI data tended to overestimate lower levels of pH1N1 incidence rates, as did the

LAB data to a lesser extent, while the product of ILI and LAB data had the strongest correlation with pH1N1 incidence rates.

Using age-standardized pH1N1 incidence rates as the proxy of influenza activity, we estimated that the overall number of excess deaths associated with the first wave of pH1N1 was 232 (95% confidence interval, CI: 136-328) under the time series regression model with most of the excess deaths in the elderly (Table 1, Table S1). Estimates of excess deaths were similar in each of the four regression models (Table 1, Table S1). Estimates of excess mortality based on proxy measures of influenza activity gave similar estimates to those based on estimated pH1N1 incidence rates (Table 1, Table S1). In comparison, there were 54 deaths in patients with laboratory-confirmed pH1N1 before 31 December 2009 (7). In sensitivity analyses, point estimates of the excess deaths were lower when influenza activity was lagged by 2 weeks and when it was not lagged (Table S2).

Based on deaths of patients with laboratory-confirmed pH1N1, point estimates of the IFRc increased with age from 0.4 to 164 deaths per 100,000 infections for individuals 5-14y to 60-69y (Table 2). Similarly, based on estimated excess deaths by the time series regression model using age-standardized incidence rates as the proxy measure of influenza activity, point estimates of the IFRe increased from approximately zero (point estimate -1.1; 95% CI: -6.1, 4.2) deaths per 100,000 infections in 5-14y to 1,100 (95% CI: 180, 4,700) deaths per 100,000 infections in 60-69y.

DISCUSSION

We estimated that during the first wave of the pandemic, pH1N1 was associated with 232 excess deaths in individuals in all ages, mostly in the elderly (Table 2). In the elderly, we estimated that there were around 10 times as many excess deaths as deaths in patients with confirmed pH1N1 (21). Although the population-wide estimate involves large standard error due to overall small age-specific estimates and large variations in the estimates by age-group, previous estimates of the excess mortality associated with pH1N1 in Hong Kong were similar to those presented here (7). Excess deaths typically exceed confirmed deaths because some deaths occur in individuals who do not present to the health-care system, while others occur in patients who are only tested for pH1N1 after cessation of detectable viral shedding or who never receive a laboratory test (3-6). In particular, excess influenza deaths in the elderly tend to exceed confirmed deaths because of non-specific presentation of influenza infections, and the association with non-respiratory causes of deaths in this age group (22, 23).

Although caution must be exercised in attempting causal interpretation of statistical estimates of excess deaths due to their ecologic nature, four different statistical methods each gave similar estimates of the excess deaths associated with pH1N1 (Table 1). The ILI×LAB proxy, a measure of the proportion of ILI due to pH1N1 among outpatients, was highly correlated with the estimated incidence

rates of pH1N1 infection suggesting that it may be a better proxy of influenza activity than either the ILI or LAB data alone (Figure 2) (24, 25).

Using estimates of the excess deaths and the cumulative incidence of infection, we found that the risk of death on a per-infection basis increased substantially with age, with the IFRe varying from below 1 per 100,000 infections in children to the order of 1,100 per 100,000 infections in those 60-69y. Combining information from a serologic study in the Netherlands (26) with excess death estimates (21), it is possible to obtain very similar estimates of the IFRe, varying from 2.1 to 2,900 deaths per 100,000 infections for individuals 5-24y to 65-74y. While incidence of infection was very low in the elderly, probably due to pre-existing immunity associated with historical exposures to similar viruses (27), we found that the high severity in this age group led to a substantial impact on mortality (Table 2). We did not identify substantial differences between IFRc and IFRe for individuals below the age of 60.

Other studies provided a wide range of estimates of the CFR of pandemic influenza (3, 11, 19, 28-31). The earliest study of the severity of pH1N1 did not account for age, and estimated that the case fatality risk was 400 deaths per 100,000 infections (29). Another study from Mexico estimated the fatality risk varying from 3 to 30 deaths per 100,000 cases with influenza-like illness in individuals aged 1-9y and ≥70y respectively (30). In the United Kingdom, the infection fatality risk was estimated to range from 5 to 9 deaths per 100,000 infections for all ages (28). Studies on previous influenza pandemics in 1918,

1957 and 1968 estimated the fatality risk among clinically apparent illnesses to be 100-2,500 per 100,000 patients (31). However, estimates of the cumulative incidence of symptomatic infection are likely to vary depending on the case definition as well as health-care seeking behaviors and surveillance systems. The IFRe measured by using cumulative incidence of infection derived from the serologic data as the denominator, and statistically-estimated deaths as the numerator, may provide a more consistent and less biased approach for comparatively assessing the severity of infection than CFR estimates.

Our study has a few limitations. First, estimates of IFRe may not be comparable between populations because the severity of infection could be affected by virus mutations, environmental conditions or host factors which may vary in different countries (32). In addition, estimates of the number of excess deaths may be zero or even negative due to harvesting or virus interference (33, 34), and in the presence of stronger such effects the IFRe may not fully capture the risk of mortality associated with influenza infection. Second, the ILI and laboratory surveillance systems in Hong Kong are not population-based, while the laboratory specimens are mostly diagnostic specimens submitted by hospitals rather than routinely collected through the ILI network. Nevertheless, ILI×LAB was highly correlated with pH1N1 incidence rates (Figure 2). Third, it is unclear whether serologic surveillance accurately measures the actual cumulative incidence in the population, because serum samples may not be collected from a representative sample of the population, and also because the validity and reliability of using seropositivity or seroconversion as indicators of infection has

yet to be explored in detail. Finally, individuals who died would not have had a chance to seroconvert and would not be reflected in the IFR denominator. This would be a relevant consideration for studies of diseases with much greater severity than pH1N1.

REFERENCES

1. Van Kerkhove MD, Asikainen T, Becker NG, et al. Studies needed to address public health challenges of the 2009 H1N1 influenza pandemic: insights from modeling. *PLoS Med* 2010;7(6):e1000275. (doi:10.1371/journal.pmed.1000275).
2. Nishiura H. Case fatality ratio of pandemic influenza. *Lancet Infect Dis* 2010;10(7):443-444. (doi:10.1016/S1473-3099(10)70120-1).
3. Wu JT, Ma ES, Lee CK, et al. The infection attack rate and severity of 2009 pandemic H1N1 influenza in Hong Kong. *Clin Infect Dis* 2010;51(10):1184-1191. (doi:10.1086/656740).
4. Warren-Gash C, Bhaskaran K, Hayward A, et al. Circulating influenza virus, climatic factors, and acute myocardial infarction: a time series study in England and Wales and Hong Kong. *J Infect Dis* 2011;203(12):1710-1718. (doi:10.1093/infdis/jir171).
5. Thompson WW, Moore MR, Weintraub E, et al. Estimating influenza-associated deaths in the United States. *Am J Public Health* 2009;99 Suppl 2:S225-230. (doi:10.2105/AJPH.2008.151944).
6. Charu V, Chowell G, Palacio Mejia LS, et al. Mortality burden of the A/H1N1 pandemic in Mexico: a comparison of deaths and years of life lost to seasonal influenza. *Clin Infect Dis* 2011;53(10):985-993. (doi:10.1093/cid/cir644).
7. Yang L, Chan KP, Cowling BJ, et al. Excess mortality associated with the 2009 pandemic of influenza A(H1N1) in Hong Kong. *Epidemiol Infect* 2011

[Available online ahead of print November 15, 2011]. (doi:10.1017/S0950268811002238).

8. Hardelid P, Pebody R, Andrews N. Mortality caused by influenza and respiratory syncytial virus by age group in England and Wales 1999-2010. *Influenza and other respiratory viruses* 2012 [Available online ahead of print March 9, 2012]. (doi:10.1111/j.1750-2659.2012.00345.x).

9. Thompson WW, Shay DK, Weintraub E, et al. Mortality associated with influenza and respiratory syncytial virus in the United States. *JAMA* 2003;289(2):179-186.

10. Lipsitch M, Hayden FG, Cowling BJ, et al. How to maintain surveillance for novel influenza A H1N1 when there are too many cases to count. *Lancet* 2009;374(9696):1209-1211. (doi:10.1016/S0140-6736(09)61377-5).

11. Presanis AM, De Angelis D, Hagy A, et al. The severity of pandemic H1N1 influenza in the United States, from April to July 2009: a Bayesian analysis. *PLoS Med* 2009;6(12):e1000207. (doi:10.1371/journal.pmed.1000207).

12. Baguelin M, Hoek AJ, Jit M, et al. Vaccination against pandemic influenza A/H1N1v in England: a real-time economic evaluation. *Vaccine* 2010;28(12):2370-2384. (doi:10.1016/j.vaccine.2010.01.002).

13. Lipsitch M, Riley S, Cauchemez S, et al. Managing and reducing uncertainty in an emerging influenza pandemic. *N Engl J Med* 2009;361(2):112-115. (doi:10.1056/NEJMp0904380).

14. Census and Statistics Department. Population and vital events. Hong Kong Special Administrative Region, China: Census and Statistics Department.

(http://www.censtatd.gov.hk/hong_kong_statistics/statistics_by_subject/). (Accessed Jan 1, 2012).

15. Department of Health. Vital statistics. Hong Kong Special Administration Region, China: Department of Health; 2011. (http://www.healthyhk.gov.hk/phisweb/en/enquiry/index.html). (Accessed Jan 1, 2012).

16. Centre for Health Protection. Sentinel surveillance. Hong Kong Special Administrative Region, China: Centre for Health Protection. (http://www.chp.gov.hk/en/dns_submenu/10/26/44.html). (Accessed Jan 1, 2012).

17. Hong Kong Observatory. Climatological information services. Hong Kong Special Administrative Region, China: Hong Kong Observatory. (http://www.hko.gov.hk/cis/climat_e.htm#). (Accessed Jan 1, 2012).

18. Wu JT, Ho A, Ma ES, et al. Estimating infection attack rates and severity in real time during an influenza pandemic: analysis of serial cross-sectional serologic surveillance data. *PLoS Med* 2011;8(10):e1001103. (doi:10.1371/journal.pmed.1001103).

19. Riley S, Kwok KO, Wu KM, et al. Epidemiological characteristics of 2009 (H1N1) pandemic influenza based on paired sera from a longitudinal community cohort study. *PLoS Med* 2011;8(6):e1000442. (doi:10.1371/journal.pmed.1000442).

20. R Development Core Team. R: A language and environment for statistical computing. 2005, R Foundation for Statistical Computing, Vienna, Austria. (http://www.R-project.org).

21. van den Wijngaard CC, van Asten L, Koopmans MPG, et al. Comparing pandemic to seasonal influenza mortality: moderate impact overall but high mortality in young children. *PLoS ONE* 2012;7(2):e31197. (doi:10.1371/journal.pone.0031197).

22. Finelli L, Chaves SS. Influenza and acute myocardial infarction. *J Infect Dis* 2011;203(12):1701-1704. (doi:10.1093/infdis/jir175).

23. Simonsen L, Clarke MJ, Williamson GD, et al. The impact of influenza epidemics on mortality: introducing a severity index. *Am J Public Health* 1997;87(12):1944-1950.

24. Goldstein E, Cobey S, Takahashi S, et al. Predicting the epidemic sizes of influenza A/H1N1, A/H3N2, and B: a statistical method. *PLoS Med* 2011;8(7):e1001051. (doi:10.1371/journal.pmed.1001051).

25. Goldstein E, Viboud C, Charu V, et al. Improving the estimation of influenza-related mortality over a seasonal baseline. *Epidemiology* 2012 (in press).

26. Steens A, Waaijenborg S, Teunis PF, et al. Age-dependent patterns of infection and severity explaining the low impact of 2009 influenza A (H1N1): evidence from serial serologic surveys in the Netherlands. *Am J Epidemiol* 2011;174(11):1307-1315. (doi:10.1093/aje/kwr245).

27. Hancock K, Veguilla V, Lu X, et al. Cross-reactive antibody responses to the 2009 pandemic H1N1 influenza virus. *N Engl J Med* 2009;361(20):1945-1952. (doi:10.1056/NEJMoa0906453).

28. Presanis AM, Pebody RG, Paterson BJ, et al. Changes in severity of 2009 pandemic A/H1N1 influenza in England: a Bayesian evidence synthesis. *BMJ* 2011;343:d5408. (doi:10.1136/bmj.d5408).

29. Fraser C, Donnelly CA, Cauchemez S, et al. Pandemic Potential of a Strain of Influenza A (H1N1): Early Findings. *Science* 2009;324(5934):1557-1561.

30. Echevarria-Zuno S, Mejia-Arangure JM, Mar-Obeso AJ, et al. Infection and death from influenza A H1N1 virus in Mexico: a retrospective analysis. *Lancet* 2009;374(9707):2072-2079. (doi:10.1016/S0140-6736(09)61638-X).

31. Taubenberger JK, Morens DM. 1918 Influenza: the mother of all pandemics. *Emerg Infect Dis* 2006;12(1):15-22.

32. Van Kerkhove MD, Vandemaele KA, Shinde V, et al. Risk factors for severe outcomes following 2009 influenza A (H1N1) infection: a global pooled analysis. *PLoS Med* 2011;8(7):e1001053. (doi:10.1371/journal.pmed.1001053).

33. Muscatello DJ, Cretikos MA, Macintyre CR. All-cause mortality during first wave of pandemic (H1N1) 2009, New South Wales, Australia, 2009. *Emerg Infect Dis* 2010;16(9):1396-1402. (doi:10.3201/eid1609.091723).

34. Cowling BJ, Fang VJ, Nishiura H, et al. Increased risk of noninfluenza respiratory virus infections associated with receipt of inactivated influenza vaccine. *Clin Infect Dis* 2012;54(12):1778-1783. (doi:10.1093/cid/cis307).

Table 1. Estimated excess all-cause deaths in Hong Kong in 2009 by 4 statistical methods and 4 measures of influenza activity, assuming a 1-week lag between influenza incidence and death.

Age	Statistical model	Influenza incidence proxy							
		Age-standardized incidence proxy		ILI×LAB		ILI		LAB	
		No.	(95% CI)	No.	(95% CI)	No.	(95% CI)	No.	(95% CI)
<60y	Time series regression	2	(-57, 61)	-15	(-72, 42)	-19	(-79, 42)	-1	(-62, 59)
	Linear regression	19	(-18, 55)	-1	(-37, 36)	9	(-27, 45)	21	(-16, 57)
	Poisson regression with log link	9	(-23, 42)	-8	(-41, 25)	-7	(-39, 26)	8	(-25, 40)
	Poisson regression with identity link	16	(-18, 50)	-3	(-37, 31)	7	(-26, 41)	18	(-16, 52)
≥60y	Time series regression	231	(154, 307)	223	(149, 298)	162	(84, 240)	201	(123, 279)
	Linear regression	230	(128, 333)	223	(120, 326)	160	(58, 263)	200	(98, 302)
	Poisson regression with log link	230	(154, 307)	221	(144, 298)	161	(85, 237)	197	(121, 273)
	Poisson regression with identity link	248	(169, 326)	236	(158, 315)	192	(115, 270)	224	(146, 302)

Abbreviations: ILI = influenza-like illness based on general practitioners (GP) consultations; LAB = laboratory specimens positive for influenza; ILI×LAB = GP consultations associated with influenza.

Table 2. Severity profile of pH1N1 during the first wave in Hong Kong in 2009.

Age	Population	CII (%)	(95% CI)	Confirmed deaths	IFRc[a]	(95% CI)	Estimated deaths	IFRe[a]	(95% CI)
0-4	229,200	na		0	na		-8	na	
5-14	644,200	43.5	(39.6, 48.3)	1	0.4	(0, 1.1)	-3	-1.1	(-6.1, 4.2)
15-29	1,430,500	16.9	(12.4, 21.3)	4	1.7	(0.3, 3.8)	2	0.8	(-12.3, 14.6)
30-39	1,114,500	5.8	(3.1, 9.7)	7	10.8	(3.6, 25.5)	2	3.1	(-40.1, 43.7)
40-49	1,273,000	3.8	(1.1, 7.5)	6	12.5	(3.4, 51.4)	8	16.7	(-51.2, 119)
50-59	1,085,400	5.0	(2.4, 8.3)	15	27.9	(14.6, 61.7)	1	1.9	(-59.2, 49.9)
60-69	555,500	0.8	(0.2, 4.2)	7	164	(18, 741)	47	1,099	(176, 4,657)
≥70	671,400	na		14	na		184	na	

Abbreviations: CII = cumulative incidence of infection (%) based on serologic surveillance studies (18, 19); IFRc = infection fatality risk based on deaths of confirmed cases; IFRe = infection fatality risk based on excess influenza-associated deaths; CI = confidence interval; na = not available.

[a] Infection fatality risks (IFR) are expressed as number of deaths per 100,000 infections. IFRc, the infection fatality risk with the numerator given by deaths among confirmed cases. IFRe, the infection fatality risk with the numerator given by the number of excess deaths. The denominator for IFRc and IFRe was the number of estimated pH1N1 infections in each age group. A bootstrap method was employed to compute 95% confidence intervals. IFRc = deaths in confirmed cases / (CII × Population) × 100,000. IFRe = estimated excess deaths / (CII × Population) × 100,000.

FIGURE LEGENDS

Figure 1. All-cause deaths, pH1N1 hospitalizations and deaths, and estimated pH1N1 incidence rates in Hong Kong, 2009. A) Weekly number of all-cause deaths. B) Weekly number of hospitalizations of patients with confirmed pH1N1. C) Weekly number of deaths of patients with confirmed pH1N1. D) Age-specific estimated incidence rates of pH1N1 infection, estimated by deconvoluting hospital admission rates and scaling to serologic surveillance data. Incidence rates by age group (5-14y (gray dot-dash), 15-19y (gray long-dash), 20-29y (gray double-dash), 30-39y (gray solid), 40-49y (gray dashed), and 50-59y (gray dotted), respectively), and the age-standardized incidence rates (black solid), expressed as rates per 100,000 population per week. Incidence rates were standardized to the local Hong Kong population.

Figure 2. Correlation between influenza-like illness (ILI) surveillance data, laboratory detection (LAB) data, and age-standardized incidence rate estimates (per 100,000 population per week) based on hospital admissions and serologic surveillance data in Hong Kong, 2009. A) Correlation between ILI based on general practitioners (GP) and incidence rates. B) Correlation between LAB data and incidence rates. C) Correlation between ILI×LAB and incidence rates. In each panel the solid line indicates the least squares regression line and the dotted line indicates the constrained ordinary least squares regression line through the origin. The dotted line in each panel has the intercept coefficient fixed at zero. The estimated intercept coefficients for the solid line in each panel were

estimated as follows: A) 41 (95% CI: 29, 53); B) 70 (95% CI: 37, 100); C) -1.3 (95% CI: -7.4, 4.7).

Figure 1

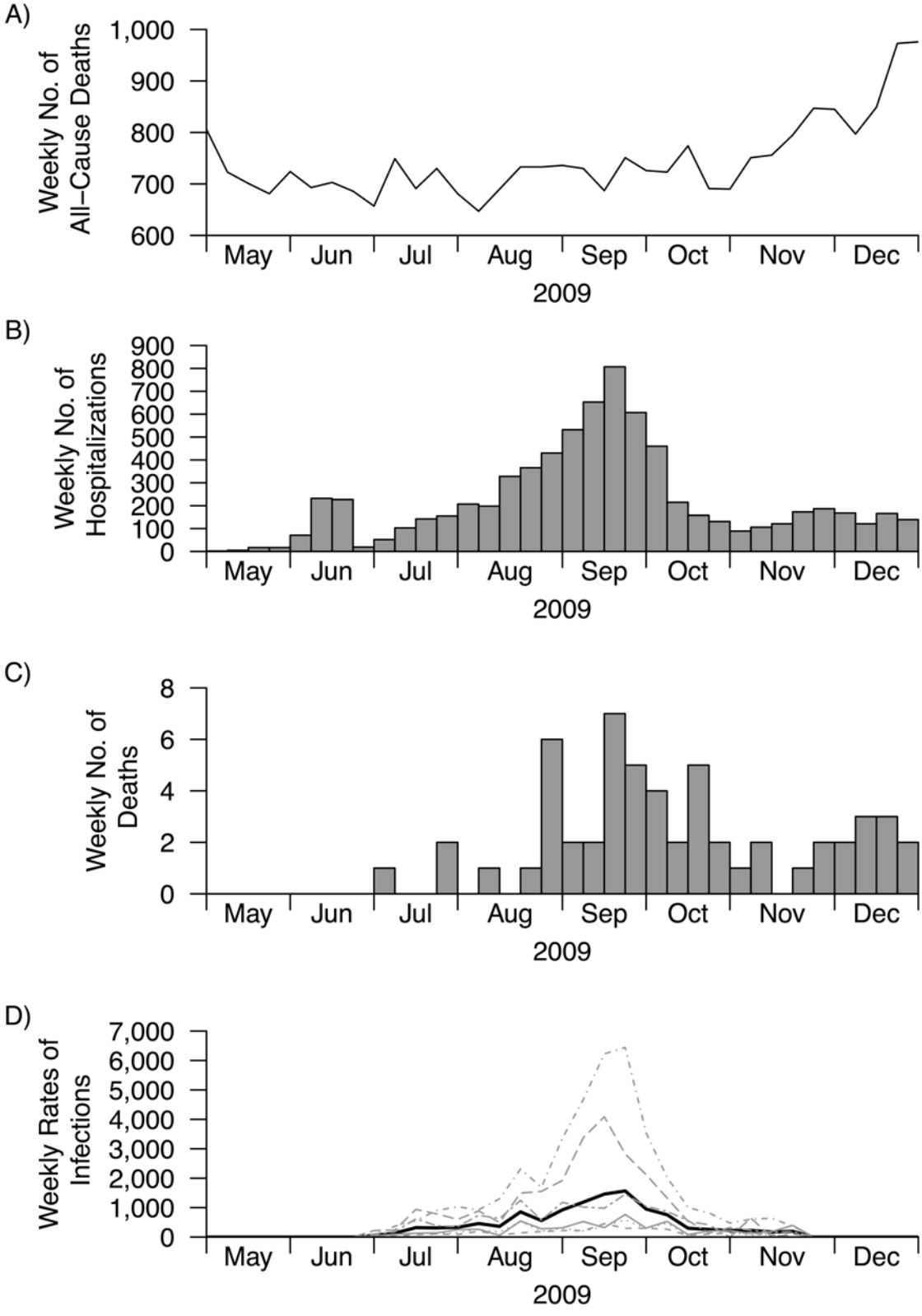
A)
Weekly No. of All–Cause Deaths
1,000
900
800
700
600
May
Jun
Jul
Aug
Sep
Oct
Nov
Dec
2009
B)
Weekly No. of Hospitalizations
900
800
700
600
500
400
300
200
100
0
May
Jun
Jul
Aug
Sep
Oct
Nov
Dec
2009
C)
Weekly No. of Deaths
8
6
4
2
0
May
Jun
Jul
Aug
Sep
Oct
Nov
Dec
2009
D)
Weekly Rates of Infections
7,000
6,000
5,000
4,000
3,000
2,000
1,000
0
May
Jun
Jul
Aug
Sep
Oct
Nov
Dec
2009

Figure 2

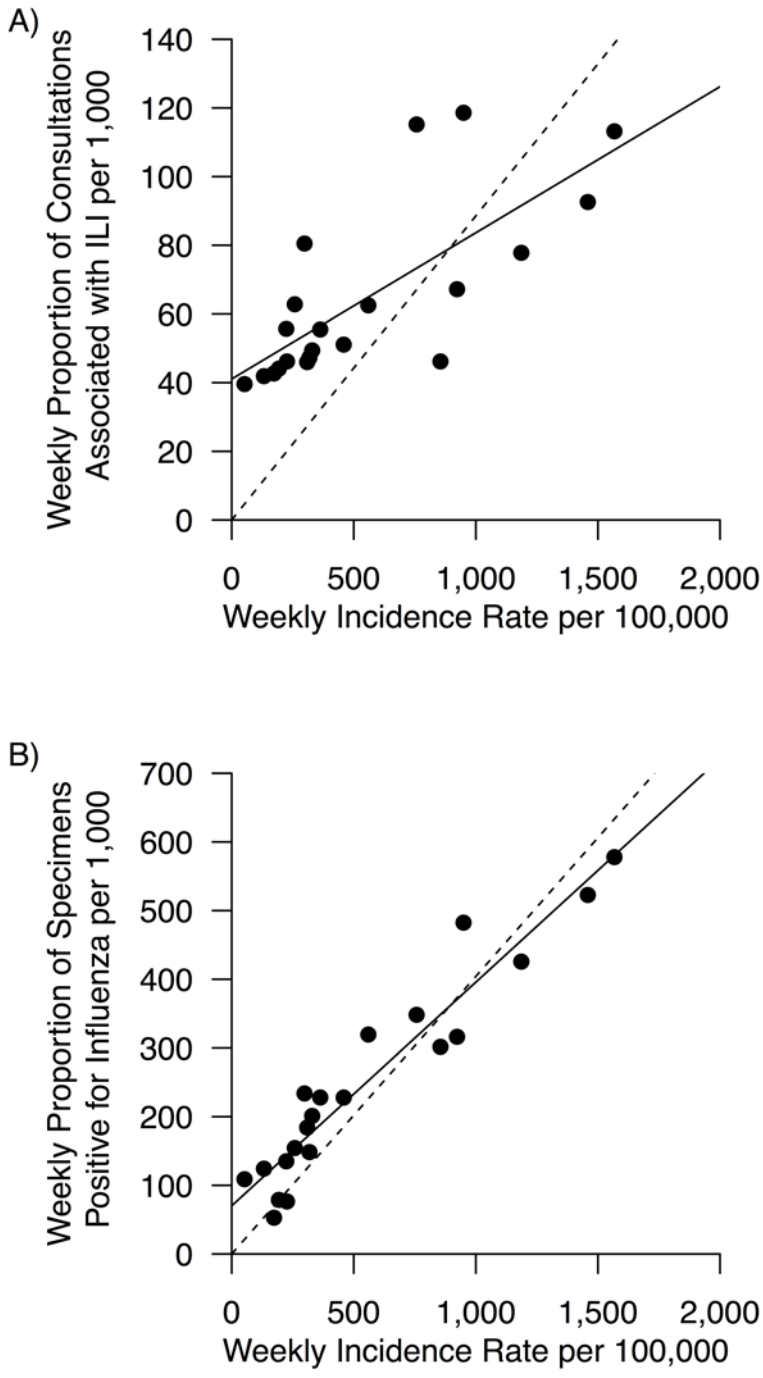
A)
Weekly Proportion of Consultations Associated with ILI per 1,000
0
20
40
60
80
100
120
140
0
500
1,000
1,500
2,000
Weekly Incidence Rate per 100,000
B)
Weekly Proportion of Specimens Positive for Influenza per 1,000
0
100
200
300
400
500
600
700
0
500
1,000
1,500
2,000
Weekly Incidence Rate per 100,000

C)

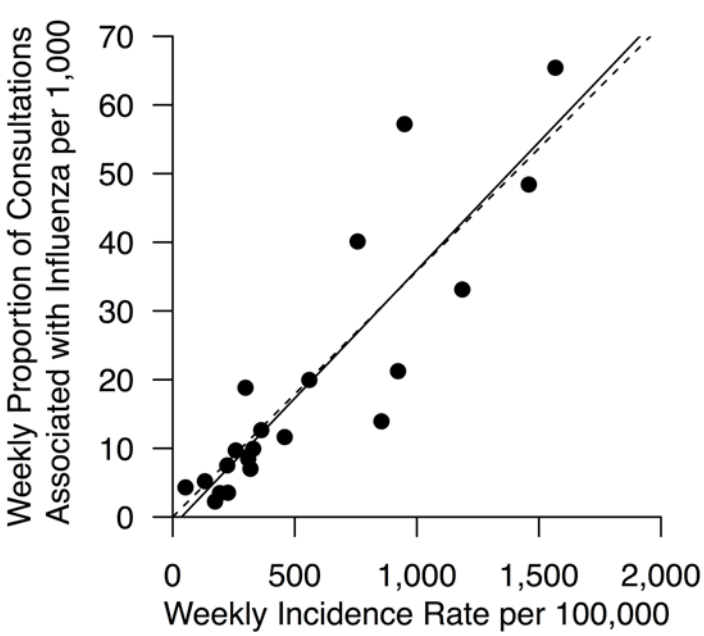
Weekly Proportion of Consultations Associated with Influenza per 1,000
70
60
50
40
30
20
10
0
0
500
1,000
1,500
2,000
Weekly Incidence Rate per 100,000

Table S1. Age-breakdown of excess all-cause deaths by 4 statistical methods and 4 measures of influenza activity, assuming a 1-week lag between influenza incidence and death.

	Influenza incidence proxy							
	Age-standardized incidence proxy		ILI×LAB		ILI		LAB	
	No.	(95% CI)	No.	(95% CI)	No.	(95% CI)	No.	(95% CI)
By time series regression model								
0-4y	-8	(-13, -3)	-6	(-11, 0)	-12	(-18, -7)	-9	(-15, -4)
5-14y	-3	(-17, 12)	-2	(-16, 13)	-1	(-16, 14)	-3	(-19, 12)
15-29y	2	(-31, 35)	1	(-30, 33)	7	(-26, 41)	3	(-31, 36)
30-39y	2	(-23, 28)	0	(-24, 25)	5	(-21, 31)	3	(-24, 29)
40-49y	8	(-22, 37)	-3	(-31, 25)	13	(-17, 43)	11	(-19, 41)
50-59y	1	(-24, 26)	-7	(-31, 17)	-31	(-56, -5)	-5	(-31, 20)
60-69y	47	(22, 72)	43	(19, 68)	63	(37, 88)	63	(38, 88)
≥70y	184	(112, 256)	180	(110, 250)	99	(26, 173)	138	(65, 211)
Overall	232	(136, 328)	208	(114, 302)	143	(45, 242)	200	(101, 298)
By linear regression model								
0-4y	-8	(-14, -3)	-6	(-11, -1)	-13	(-18, -7)	-9	(-15, -4)
5-14y	-3	(-6, 0)	-2	(-5, 1)	-1	(-4, 2)	-3	(-7, 0)
15-29y	6	(-3, 15)	5	(-5, 14)	13	(4, 23)	8	(-1, 17)
30-39y	3	(-6, 12)	1	(-8, 10)	6	(-4, 15)	3	(-6, 13)
40-49y	15	(-2, 33)	4	(-13, 22)	25	(7, 42)	21	(3, 38)

50-59y	6	(-23, 34)	-3	(-31, 26)	-21	(-49, 8)	2	(-27, 30)
60-69y	46	(13, 80)	43	(9, 76)	62	(28, 95)	62	(29, 95)
≥70y	184	(87, 281)	180	(83, 277)	99	(2, 196)	138	(41, 234)
Overall	249	(140, 358)	222	(113, 331)	170	(61, 278)	221	(112, 329)
By Poisson regression model with log link								
0-4y	-8	(-14, -3)	-6	(-11, 0)	-12	(-17, -7)	-9	(-14, -4)
5-14y	-3	(-6, -1)	-2	(-4, 1)	-2	(-4, 1)	-4	(-6, -1)
15-29y	2	(-5, 8)	1	(-6, 8)	7	(-1, 14)	2	(-5, 9)
30-39y	2	(-7, 12)	0	(-9, 10)	5	(-5, 14)	3	(-7, 12)
40-49y	13	(-3, 28)	2	(-14, 18)	20	(4, 35)	17	(1, 32)
50-59y	4	(-21, 30)	-4	(-30, 21)	-24	(-49, 1)	-1	(-26, 25)
60-69y	33	(5, 61)	31	(3, 59)	42	(14, 70)	44	(16, 72)
≥70y	197	(126, 268)	190	(118, 261)	119	(48, 190)	153	(82, 224)
Overall	240	(157, 323)	213	(130, 297)	155	(72, 237)	205	(112, 288)
By Poisson regression model with identity link								
0-4y	-9	(-14, -4)	-6	(-11, 0)	-12	(-17, -7)	-9	(-14, -4)
5-14y	-4	(-6, -1)	-2	(-5, 0)	-2	(-5, 1)	-5	(-7, -2)
15-29y	5	(-3, 13)	4	(-4, 12)	12	(4, 20)	7	(-1, 15)
30-39y	2	(-2, 31)	0	(-10, 11)	5	(-5, 15)	3	(-7, 13)
40-49y	15	(-20, 32)	3	(-13, 20)	25	(-9, 42)	21	(5, 38)
50-59y	6	(17, 77)	-3	(-29, 23)	-21	(-47, 5)	1	(-25, 27)

60-69y	47	(17, 77)	44	(14, 74)	65	(35, 94)	64	(34, 94)
≥70y	201	(129, 273)	193	(120, 265)	128	(56, 200)	160	(88, 232)
Overall	264	(179, 349)	233	(148, 319)	200	(115, 285)	243	(158, 327)

ILI = influenza like illness based on general practitioners (GP) consultations; LAB = laboratory specimens positive for influenza; ILI×LAB = GP consultations associated with influenza.

Table S2. Estimated overall excess all-cause deaths by 4 statistical methods and 4 measures of influenza activity, assuming 0-week and 2-week lags between influenza incidence and death.

Lag	Statistical model	Influenza incidence proxy							
		Age-standardized incidence proxy		ILI×LAB		ILI		LAB	
		No.	(95% CI)	No.	(95% CI)	No.	(95% CI)	No.	(95% CI)
No lag	Time series regression	109	(-3, 221)	136	(27, 245)	19	(-96, 134)	76	(-38, 191)
	Linear regression	125	(-9, 259)	149	(15, 284)	43	(-91, 176)	95	(-38, 229)
	Poisson regression with log link	120	(37, 202)	141	(58, 225)	31	(-52, 113)	85	(3, 168)
	Poisson regression with identity link	150	(65, 236)	169	(83, 255)	83	(-2, 168)	130	(46, 215)
2-week lag	Time series regression	145	(36, 255)	125	(18, 232)	33	(-79, 145)	119	(7, 231)
	Linear regression	164	(35, 294)	141	(10, 271)	60	(-69, 190)	141	(12, 271)
	Poisson regression with log link	156	(73, 240)	131	(47, 215)	49	(-34, 132)	128	(45, 211)
	Poisson regression with identity link	181	(96, 266)	153	(68, 239)	95	(10, 180)	168	(83, 253)

ILI = influenza like illness based on general practitioners (GP) consultations; LAB = laboratory specimens positive for influenza; ILI×LAB = GP consultations associated with influenza.

WEB APPENDIX

The infection fatality risk of pandemic influenza A(H1N1) in Hong Kong in 2009

This appendix provides additional information on the data and statistical methods used.

1. MEASURES OF INFLUENZA ACTIVITY

1.1 Incidence rates of pH1N1 infection

In a serologic study, we collected approximately 13,000 serum specimens during the first wave of the 2009 pandemic in Hong Kong (1). We obtained the specimens from three groups of individuals including: (1) Blood donors (16-59y) participating in the Hong Kong Red Cross Blood Transfusion Service; (2) Patients (5-90y) visiting the Pediatric and Adolescent Medicine outpatient clinic and the Medicine outpatient clinic at Queen Mary Hospital, a local tertiary care centre; (3) Subjects aged 5-14y in a community-based cohort study. The majority of sera came from blood donors and in detailed analysis we found no difference in estimates of the cumulative incidence of infection from each source (2).

We used a "deconvolution" approach to estimate incidence rates of pH1N1 infection from the serologic surveillance data and hospital admission rates (see Figure 3 in (1)). In brief, we obtained unscaled incidence rates of pH1N1 infection by deconvoluting the time series of hospitalizations associated with pH1N1 accounting for the delay from infection to hospitalization. Then we estimated unscaled seropositivity fractions over time (defined as the proportion that had microneutralization titer at or above 1:40 at a given point in calendar

time) from the unscaled incidence rates of pH1N1 infection accounting for the delay from infection to seropositivity. Lastly, we scaled the incidence rates of pH1N1 infection by fitting the unscaled seropositivity rates to the serologic surveillance data (1).

1.2 Influenza-like illness and laboratory surveillance data

We used influenza-like illness (ILI) data on the proportion of outpatients with ILI among all outpatient visits from a network of sentinel general practitioners in the private sector in Hong Kong (Web Figure 1). ILI is defined as body temperature >37.8°C with cough or sore throat. The sentinel network has included around 50 private outpatient clinics since its creation in 1998. Around 70% of outpatient consultations occur in the private sector in Hong Kong (3). A separate network also reports similar data from clinics in the public sector, but there is a cap on walk-in attendance and data from the private network appear to be more responsive to changes in influenza activity in the community (4, 5).

We used laboratory (LAB) data on the proportion of respiratory specimens tested that were positive for a particular influenza type/subtype, including seasonal influenza A(H1N1), A(H3N2), B, and 2009 pandemic influenza A(H1N1)

(Web Figure 1). Specimens were tested using viral culture or reverse transcription polymerase chain reaction. Most specimens were provided by local hospitals for diagnostic and surveillance purposes, and some specimens were submitted by the sentinel outpatient clinics. The median number of specimens tested each week was 619 (inter-quartile range 325-819) with some seasonal variation.

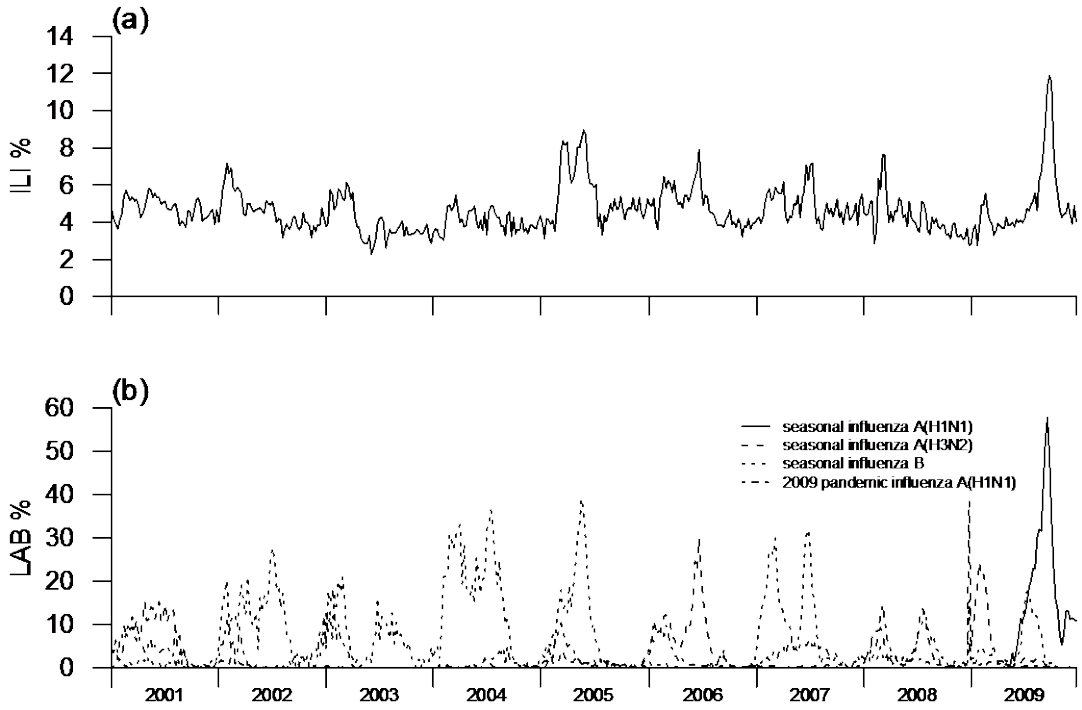

Web Figure 1. ILI and LAB data per week from 2001-09 in Hong Kong. (a) Weekly proportion of patients with influenza-like illness among all outpatient consultations in around 50 outpatient clinics. (b) Weekly proportion of laboratory specimens that tested positive for influenza by type and subtype.

2. COVARIATES

We fitted four separate types of regression model to explore the association between influenza activity and mortality, adjusting for covariates including seasonal influenza activity, respiratory syncytial virus activity, mean temperature and absolute humidity.

A series of terms representing influenza activity were included as weekly data of the form $ILI \times LAB_s$ where LAB_s is the proportion of laboratory detections of influenza type/subtypes among all specimens submitted. Similarly, respiratory syncytial virus activity was included as a term of the form $ILI \times LAB_{rsv,}$ where LAB_{rsv} is the proportion of laboratory detections of respiratory syncytial virus among all specimens submitted.

We used absolute humidity (AH) instead of relative humidity (RH) since AH has been suggested to be a better predictor of influenza infection and virus survival in previous studies (6). RH is the ratio of the partial pressure of water vapor in the air to the saturated vapor pressure of water, and expressed as a percentage. AH indicates the actual water vapor content in the air which was measured in

our study by the density of water vapor (D_w, g/m^3). The relationship between different meteorological parameters is indicated by the equations below:

$$RH = \frac{e(T)}{e_s(T)} \times 100 \quad [1]$$

$$e_s(T) = 611.2 \times \exp(\frac{17.67 \times T}{T + 243.5}) \quad [2]$$

$$D_w = \frac{M \times e(T)}{(T + 273.1) \times R_w} \quad [3]$$

where e(T) and e_s(T) refer to the partial and saturation vapor pressure at temperature T with the unit of Pascal (Pa). e_s(T) in equation [2] is an approximation (7). T is measured in Celsius in the above equations. M is the molecular weight of water vapor, 18.016 g/mol. R_w, the gas content of water vapor, approximately equals to 8.314472 Pa·m^3/mol·K.

3. STATISTICAL MODELS

We used four classes of statistical models to estimate the excess deaths associated with pH1N1, namely time series regression, linear regression, and Poisson regression models with log link and identity link. We applied each regression model to the time series of weekly all-cause death rates (Web Figure

2). The data were stratified into 8 age groups: 0-4 years, 5-14y, 15-29y, 30-39y, 40-49y, 50-59y, 60-69y and ≥70y for analysis.

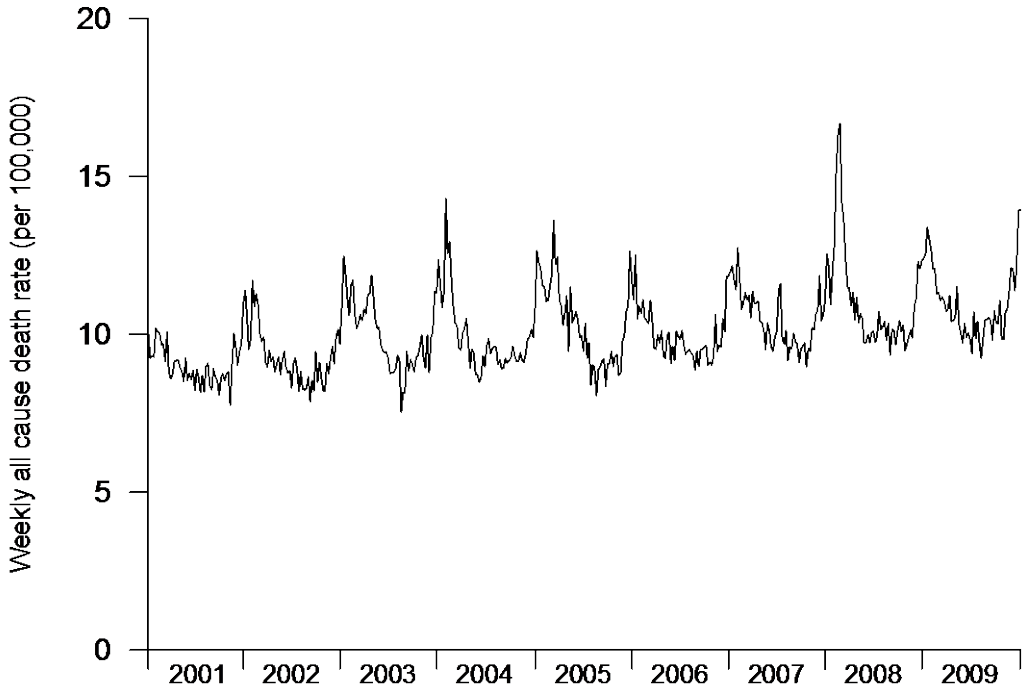

Web Figure 2: All-cause mortality rates per 100,000 population per week from 2001-09 in Hong Kong.

In each model we included a linear predictor of the form $\{\boldsymbol{\beta X_t}\}$ where $\boldsymbol{\beta}$ represents a vector of regression parameters and $\mathbf{X_t}$ is a vector of covariates.

$$\{\boldsymbol{\beta X}_t\} = \beta_1 t + \beta_2 \sin\frac{2\pi t}{52} + \beta_3 \cos\frac{2\pi t}{52} + \beta_4 \sin\frac{4\pi t}{52} + \beta_5 \cos\frac{4\pi t}{52} +$$
$$\beta_6 TEMP_{t-1} + \beta_7 TEMP_{t-1}^2 + \beta_8 TEMP_{t-1}^3 + \beta_9 HUMID_{t-1} + \beta_{10} HUMID_{t-1}^2 + \beta_{11} HUMID_{t-1}^3 +$$
$$\beta_{12} FLU_{t-1}^{sH1N1} + \beta_{13} FLU_{t-1}^{sH3N2} + \beta_{14} FLU_{t-1}^{B} + \beta_{15} RSV_{t-1} + \beta_{16} FLU_{t-1}^{pH1N1}$$

where t represents the week number, β_1 represents the regression coefficient of the linear trend of mortality, β_2-β_5 represent the regression coefficients of the seasonal variations in deaths, β_6-β_8 represent the regression coefficients of the linear and non-linear effect of temperature, β_9-β_{11} represent the regression coefficients of the linear and non-linear effect of humidity, β_{12}-β_{14} and β_{16} are the regression coefficients of the effect from the activities of different influenza types/subtypes, and β_{15} represents the regression coefficient of the effect associated with respiratory syncytial virus activity. FLU_{t-1}^{sH1N1}, FLU_{t-1}^{sH3N2}, FLU_{t-1}^{B}, FLU_{t-1}^{pH1N1} represent seasonal influenza A(H1N1), A(H3N2), B, and 2009 pandemic influenza A(H1N1) activities in week t-1 respectively since we assumed a time lag of one week between the virus activity and the caused deaths in the main model.

3.1 Age-specific time series regression model

The model is described by the following equations (8, 9):

$$\frac{D_t}{N_t} = \theta_t + \{\boldsymbol{\beta X_t}\} + \varepsilon_t, \varepsilon_t \sim N(0, \sigma_\varepsilon^2)$$

$$\theta_t = \theta_{t-1} + \zeta_t, ?\zeta_t \sim N\left(0, \sigma_\zeta^2\right)$$

where D_t represents the number of deaths in week t, and N_t represents the population size in week t. $\{\boldsymbol{\beta X_t}\}$ represents the linear predictor. θ_t represents the unobserved level in week t and ζ_t represents the level disturbance in week t, which are assumed to be independent and identically distributed random variables that follow normal distribution with zero mean and variances σ_ζ^2. In this model, the level component is allowed to vary over time. Level component at week t depends on the level at week t-1 and the level disturbance at week t.

3.2 Age-specific linear regression model with identity link

The model is described by the following equation:

$$\frac{D_t}{N_t} = \beta_0 + \{\boldsymbol{\beta X}_t\} + \varepsilon_t, \varepsilon_t \sim N(0, \sigma_\varepsilon^2)$$

where D_t represents the number of deaths in week t, N_t represents the population size in week t, and β_0 represents the intercept. $\{\boldsymbol{\beta X_t}\}$ represents the linear predictor.

3.3 Age-specific Poisson regression model with log link

The model is described by the following equation:

$$\log(E(D_t)) = \log(N_t) + \beta_0 + \{\boldsymbol{\beta X}_t\}$$

where D_t represents the number of deaths in week t, N_t represents the population size in week t, and β_0 represents the intercept. $\{\boldsymbol{\beta X_t}\}$ represents the linear predictor.

3.4 Age-specific Poisson regression model with identity link

The model is described by the following equation:

$$E(D_t) = N_t \times [\beta_0 + \{\boldsymbol{\beta X}_t\}]$$

where D_t represents the number of deaths in week t, N_t represents the population size in week t, and β_0 represents the intercept. $\{\boldsymbol{\beta X_t}\}$ represents the linear predictor.

3.5 Seasonality

The model considered the effect on the association between influenza activity and mortality from the model with trigonometric components of 12 months + 6 months which was found to be the best fitting model with the smallest mean squared error (MSE) defined as:

$$MSE = \frac{1}{n}\sum_{t=1}^{n}(f_t - \frac{D_t}{N_t})^2$$

where n represents the number of observations in the time series. f_t represents the one-step-ahead forecasts based on data up to week t-1. D_t represents the

number of deaths in week t, and N_t is the population size in week t. The comparison of the MSE of alternative models is shown in the Web Table 1. A similar approach was used to determine the optimal seasonal components in the other models (data not shown).

There are 53 weeks in the year 2006. We deleted week 22, which has the lowest seasonal influenza activity, to permit the model to be fitted with trigonometric components of 52 weeks across the entire study period.

Web Table 1. Model assessment by 6 combinations of trigonometric components.

Trigonometric components*	**Mean Squared Error**
12m	28.22
12m + 6m	27.56
12m + 6m + 4m	28.09
12m + 6m + 4m + 3m	28.38
12m + 6m + 4m + 3m + 2m	28.47
12m + 6m + 4m + 3m + 2m + 1m	28.81

* Trigonometric components were added to time series regression model for the ≥70y age group in which age-standardized incidence of pH1N1 was treated as the measure of influenza activity, assuming 1-week lag between influenza incidence and death.

3.6 Model checking

We assessed model fit using residuals from fitted models. No structure is left in the residuals and the estimated autocorrelation function (ACF) of the residuals for the four statistical models using age-standardized incidence rate as the proxy of influenza activity (data not shown). All models provided good fit to the data.

3.7 Confidence intervals for the influenza-associated excess mortality rates

The influenza-associated excess mortality rates were calculated by subtracting the predicted mortality rate estimated from each fitted regression model setting influenza activity as zero from the predicted mortality rate from the same model based on the observed weekly influenza activity. The confidence intervals of the influenza-associated excess mortality rates is obtained by the following steps:

Step 1: We calculated the standard error of the excess mortality rates based on standard error of the weekly baseline mortality rates and standard error of weekly observed mortality rates, which is described by the following equation:

$$SE^T = \sqrt{\sum_{t=1}^{n} (SE_t^B)^2 + (SE_t^O)^2}$$

where n represents the number of observations in the time series,

SE^T represents the standard error (SE) of the total weekly excess mortality

rates, SE^B represents the SE of the weekly baseline mortality rates in week t, and SE^O represents the SE of the weekly observed mortality rates in week t.

Step 2: We calculated the confidence intervals of the excess mortality rates based on the standard error of the excess mortality rates (obtained from step 1). To obtain the upper limit, we multiplied the standard error by 1.96 and added it to the excess mortality rates to. Similarly, subtracting to obtain the lower limit.

4. CUMULATIVE INCIDENCE OF INFECTION

Age-specific estimates of the cumulative incidence of infection (CII) in the first wave were estimated in separate serologic surveillance studies (1, 10), and used as the denominators for estimation of IFRc and IFRe. During the first wave of the 2009 pandemic in Hong Kong, Wu et al. conducted a serial cross-sectional serologic study (1) and obtained serum specimens from three groups of individuals including blood donors (16-59y), hospital outpatients (5-90y), and participants of a community pediatric cohort study (5-14y). Riley et al. conducted a paired serologic study during the same period in Hong Kong. They obtained serum specimens from a cohort of households (3-103y), recruited from the community by random digit dialing to their home telephone numbers. Pre-

pandemic sera were collected between July and September 2009 and post-pandemic sera were collected from November 2009 to January 2010. Estimates of the cumulative incidence of infection were corrected for the non-bracketing design (10). In both studies, the age-specific CII estimates were very similar (1, 10).

We derived the CII for individuals aged 5-14y, 15-29y, 30-39y, 40-49y and 50-59y based on Wu et al. (1). For individuals aged 60-69y, we used the estimate from Riley et al. for individuals aged ≥60y (10) in our analysis because only 34% of individuals in the ≥60y age group in that study were older than 70y. We did not have sufficient data to estimate the CII for individuals 0-4y and ≥70y.

5. INFECTION FATALITY RISK

In the present study, we proposed a severity measure referred to as the infection fatality risk (IFR), and define it as the number of influenza-associated deaths divided by the number of infections in a population or subgroup.

5.1 IFRc and IFRe

We investigated the IFR where the numerator is based on deaths among individuals with confirmed pH1N1 infection (abbreviated IFRc) as well as with the numerator based on statistical estimates of excess deaths associated with pH1N1 (abbreviated IFRe). The denominator for IFRc and IFRe was the number of estimated pH1N1 infections in each subgroup. The IFRc and IFRe defined as:

$$INF = CII \times N \quad [4]$$

$$IFRc = \frac{D^c}{INF} \times 100000 \quad [5]$$

$$IFRe = \frac{D^e}{INF} \times 100000 \quad [6]$$

where INF refer the number of estimated pH1N1 infections, CII represents the cumulative incidence of infection, N represents the population size, D^c represents the deaths among individuals with confirmed pH1N1 infection, and D^e represents the statistical estimates of excess deaths associated with pH1N1.

5.2 Confidence intervals for the infection fatality risk

A bootstrap method was employed to compute 95% confidence intervals with the following steps:

For IFRc:

Step 1: From the sampling distribution of the confirmed deaths (D^c) we generated 1000 bootstrap samples, D_i^c i=1,2,...,1000.

Step 2: From the sampling distribution of the number of estimated pH1N1 infections (INF) we generated 1000 bootstrap samples, INF_i i=1,2,...,1000.

Step 3: We calculated 1000 samples of IFRc by equation [5] using the 1000 samples of D^c (step 1) pairwise divided by the 1000 samples of INF (step 2), $IFRc_i$ i=1,2,...,1000.

Step 4: We obtained the 95% bootstrap confidence interval for IFRc as the 2.5 and 97.5 percentiles of the 1000 bootstrap samples of IFRc from step 3.

For IFRe:

Step 1: From the sampling distribution of the estimated excess deaths (D^e) we generated 1000 bootstrap samples, D_i^e i=1,2,...,1000.

Step 2: From the sampling distribution of the number of estimated pH1N1 infections (INF) we generated 1000 bootstrap samples, INF_i i=1,2,...,1000.

Step 3: We generated 1000 samples $IFRe_i$ i=1,2,...,1000 via equation [6] by pairwise division of the 1000 samples of D^e (step 1) and the 1000 samples of INF (step 2),

Step 4: We obtained the 95% bootstrap confidence interval for IFRe as the 2.5 and 97.5 percentiles of the 1000 bootstrap samples of IFRe from step 3.

APPENDIX REFERENCES

1. Wu JT, Ho A, Ma ES, et al. Estimating infection attack rates and severity in real time during an influenza pandemic: analysis of serial cross-sectional serologic surveillance data. *PLoS Med* 2011;8(10):e1001103. (doi:10.1371/journal.pmed.1001103).
2. Wu JT, Ma ES, Lee CK, et al. The infection attack rate and severity of 2009 pandemic H1N1 influenza in Hong Kong. *Clin Infect Dis* 2010;51(10):1184-1191. (doi:10.1086/656740).
3. Leung GM, Wong IO, Chan WS, et al. The ecology of health care in Hong Kong. *Soc Sci Med* 2005;61(3):577-590. (doi:10.1016/j.socscimed.2004.12.029).
4. Cowling BJ, Wong IO, Ho LM, et al. Methods for monitoring influenza surveillance data. *Int J Epidemiol* 2006;35(5):1314-1321. (doi:10.1093/ije/dyl162).
5. Lau EH, Cowling BJ, Ho LM, et al. Optimizing use of multistream influenza sentinel surveillance data. *Emerg Infect Dis* 2008;14(7):1154-1157.
6. Shaman J, Kohn M. Absolute humidity modulates influenza survival, transmission, and seasonality. *Proceedings of the National Academy of Sciences of the United States of America* 2009;106(9):3243-3248. (doi:10.1073/pnas.0806852106).
7. National Oceanic and Atmospheric Administration of the United States Department of Commerce. Relative humidity and dewpoint temperature from temperature and wet-bulb temperature. (http://www.srh.noaa.gov/images/epz/wxcalc/rhTdFromWetBulb.pdf). (Accessed Mar 2012).
8. Commandeur JJF, Koopman SJ. *An Introduction to State Space Time Series Analysis*. Oxford, U.K: Oxford University Press; 2007.
9. Petris G, Petrone S, Campagnoli P. *Dynamic Linear Models with R*. New York: Springer Verlag; 2009.
10. Riley S, Kwok KO, Wu KM, et al. Epidemiological characteristics of 2009 (H1N1) pandemic influenza based on paired sera from a longitudinal community cohort study. *PLoS Med* 2011;8(6):e1000442. (doi:10.1371/journal.pmed.1000442).